Biophysical Journal Volume 68 May 1995 2156–2170

Calcium Transients In Cerebellar Granule Cell Presynaptic Terminals

Wade G. Regehr and Pradeep P. Atluri
Department of Neurobiology, Harvard Medical School, Boston, Massachusetts 02115 USA

ABSTRACT Calcium ions act presynaptically to modulate synaptic strength and to trigger neurotransmitter release. Here we detect stimulus-evoked changes in residual free calcium ($[Ca^{2+}]_i$) in rat cerebellar granule cell presynaptic terminals. Granule cell axons, known as parallel fibers, and their associated boutons, were labeled with several calcium indicators. When parallel fibers were extracellularly activated with stimulus trains, calcium accumulated in the terminals, producing changes in the fluorescence of the indicators. During the stimulus train, the fluorescence change per pulse became progressively smaller with the high affinity indicators Fura-2 and calcium green-2 but remained constant with the low affinity dyes BTC and furaptra. In addition, fluorescence transients of high affinity dyes were slower than those of low affinity indicators, which appear to accurately report the time course of calcium transients. Simulations show that differences in the observed transients can be explained by the different affinities and off rates of the fluorophores. The return of $[Ca^{2+}]_i$ to resting levels can be approximated by an exponential decay with a time constant of 150 ms. On the basis of the degree of saturation in the response of high affinity dyes observed during trains, we estimate that each action potential increases $[Ca^{2+}]_i$ in the terminal by several hundred nanomolar. These findings indicate that in these terminals $[Ca^{2+}]_i$ transients are much larger and faster than those observed in larger boutons, such as those at the neuromuscular junction. Such rapid $[Ca^{2+}]_i$ dynamics may be found in many of the terminals in the mammalian brain that are similar in size to parallel fiber boutons.

INTRODUCTION

Measurements of residual free calcium ($[Ca^{2+}]_i$) in presynaptic terminals have been invaluable in defining calcium's roles in synaptic transmission. It appears that presynaptic calcium controls synaptic strength in a variety of ways and on a multitude of time scales. The release of neurotransmitter is initiated by increases in calcium from resting levels of approximately 50 nM to greater than 50 μM near calcium channels opened by an action potential (Simon and Llinas, 1985; Fogelson and Zucker, 1985; Adler et al., 1991; Augustine et al., 1991; Heidelberger et al., 1994). The calcium-binding site(s) involved in this process are thought to be low affinity and rapid. In addition, modest but sustained increases in $[Ca^{2+}]_i$ produced by trains of action potentials contribute to synaptic enhancement on the tens of seconds time scale, which corresponds to processes referred to as augmentation and posttetanic potentiation (PTP) (Delaney and Tank, 1994; Delaney et al., 1989; Regehr et al., 1994; Swandulla et al., 1991). In these processes calcium must act at a high affinity site distinct from the one involved in triggering vesicle fusion. Calcium may also contribute to use-dependent enhancement on the tens of milliseconds to seconds time scale, corresponding to the first and second component of facilitation (Katz and Miledi, 1968; Yamada and Zucker, 1992; Blundon et al., 1993; Winslow et al., 1994).

To date, most of the studies that suggest that calcium has multiple actions in synaptic transmission have been performed at the squid giant synapse and the crayfish neuromuscular junction. $[Ca^{2+}]_i$ has been measured on time scales in which the calcium has equilibrated with calcium-binding proteins in the terminal, and the spatial concentration gradients near the release site have collapsed. This approach is well suited to detecting the calcium involved in PTP and augmentation. It also holds promise for the quantification of calcium entering a terminal during an action potential, although it is not suited to measuring the brief and localized calcium signal that triggers neurotransmitter release (however, see Llinas et al., 1992).

There are important reasons to extend such studies to synapses in the mammalian brain. It is likely that calcium dynamics, which have been shown to dictate the amplitude and duration of enhancement at the crayfish neuromuscular junction (Delaney and Tank, 1994; Delaney et al., 1989), will be very different in the much smaller boutons typical of the mammalian brain. In addition, accurate measurements of $[Ca^{2+}]_i$ changes in presynaptic terminals will be valuable in determining whether changes in calcium influx contribute to plasticity at synapses in the mammalian brain.

Initial studies in which $[Ca^{2+}]_i$ measurements were made in presynaptic terminals from the mammalian brain were performed at the mossy fiber synapse between granule cells and CA3 pyramidal cells in the hippocampus (Regehr et al., 1994; Regehr and Tank, 1991a,b). The presynaptic terminals of this synapse are particularly large (4–5 μm in diameter), so that it is possible to measure $[Ca^{2+}]_i$ in single boutons. The $[Ca^{2+}]_i$ dynamics in these terminals differ significantly from those in crayfish. Calcium transients are larger and decay more rapidly, consistent with theoretical predictions that the time constant of decay scales as the radius of the terminal, and the magnitudes of $[Ca^{2+}]_i$ accumulations are inversely proportional to the radius. The very features of the mossy fiber terminals that make them amenable to study differentiate them from synapses with much smaller presynaptic terminals more typical of those in the mammalian brain.

Received for publication 17 October 1994 and in final form 2 February 1995.

Address reprint requests to Dr. W. Regehr, Department of Neurobiology, Harvard Medical School, Boston, MA 02115. Tel.: 617-432-0435; Fax: 617-734-7557; E-mail: wregehr@warren.med.harvard.edu.

Extending $[Ca^{2+}]_i$ measurement techniques to terminals 1 μm in diameter poses serious challenges. It is extremely difficult to quantify $[Ca^{2+}]_i$ in individual boutons owing to their minuscule volumes. However, for small terminals it is possible to detect changes in calcium from many boutons. Such aggregate measurements have been made for the presynaptic terminals of two synapses in the hippocampus with the calcium indicator Fura-2, the mossy fiber synapse (Regehr et al., 1994; Regehr and Tank, 1991a,b), and the CA3 to CA1 pyramidal cell synapse (Wu and Saggau, 1994a,b). Aggregate measurements of Fura-2 fluorescence were similar to calcium transients measured from individual boutons for the large mossy fiber terminals (Regehr et al., 1994). However, it is not clear that Fura-2 can be used to quantify $[Ca^{2+}]_i$ in small terminals with this approach. Recent studies suggest that when calcium transients are large and fast, as in skeletal muscle (Baylor and Hollingworth, 1988; Klein et al., 1988), in myocytes (Berlin and Konishi, 1993), and in presynaptic structures in the frog tectum (Feller et al., 1993; Feller et al., submitted for publication), Fura-2 does not accurately report $[Ca^{2+}]_i$.

Here we examine presynaptic calcium transients at the synapse between cerebellar granule cells and Purkinje cells (Palay and Chan-Palay, 1974). These boutons are approximately 1 μm in diameter, similar in size to many of the boutons in the central nervous system; it is therefore likely that the findings described here will have important implications for calcium signaling in synaptic boutons in the mammalian brain. Experiments with a number of dyes with different calcium affinities indicate that single action potentials can produce large and brief changes in presynaptic calcium in terminals associated with parallel fibers. Fluorescence measurements with low affinity dyes indicate that these calcium transients decay with a time constant of ~150 ms, which is much more rapid than has been observed in mossy fiber synapses or at the crayfish neuromuscular junction. The decay time was not accurately reported by high affinity dyes such as Fura-2. The amplitudes of the calcium accumulations were found to be sufficiently large to begin to saturate the response of the high affinity dyes.

MATERIALS AND METHODS

Transverse slices (200–300 μm thick) were cut from the cerebellar vermis of 9- to 14-day-old rats. In this orientation, the parallel fibers run for several millimeters parallel to the surface of the slice in the molecular layer. The external solution (2 ml/min rate of perfusion) consisted of (in mM): 125 NaCl, 2.5 KCl, 2 $CaCl_2$, 1 $MgCl_2$, 26 $NaHCO_3$, 1.25 NaH_2PO_4, and 25 glucose, bubbled with 95% O_2 and 5% CO_2. Slices were submerged in a chamber with a volume of 1 ml. External solution supplemented with tetrodotoxin (TTX), Cd, or other agents was applied with a gravity-fed superfusion system.

Labeling procedure

Parallel fibers were labeled by local application of a solution containing the membrane-permeant form of BTC (Iatridou et al., 1994), Fura-2 (Grynkiewicz et al., 1985), furaptra (Konishi et al., 1991; Raju et al., 1989), or calcium green-2 (Molecular Probes, Eugene, OR) by a procedure that was slightly modified from that described in Regehr and Tank (1991b). In brief, 50 μg of one of these indicators were dissolved in 20 μl of 25% pluronic acid/75% dimethylsulfoxide, 400 μl of saline were added, and the solution was then vortexed for 1 min. In some experiments, fast green was also included to allow visualization of the solution in bright field. Solutions were prepared each day and used shortly thereafter. A delivery pipette of 8–15 μm in diameter was filled with labeling solution. A suction pipette of 25–30 μm was situated near the outflow of the labeling pipette to restrict the flow of the dye and prevent loading of other sites in the slice. Regulated pressure from an aquarium pump forced from the delivery pipette a jet of solution, which was collected by the suction pipette. The two pipettes were lowered together until the delivery pipette touched the slice surface, halting the flow of solution. The pressure applied to the delivery pipette was then increased slightly until dye resumed flowing. Care was taken to keep the dye confined to a small loading site. The loading time for these experiments was generally 30 min, although in some experiments the effect of loading time was checked by loading for shorter times, as indicated. With time, dye diffused within the parallel fibers, producing a fluorescent band in the molecular layer, as shown in Fig. 1.

The labeling observed with BTC and furaptra was very bright, typically more intense than with Fura-2 and calcium green-2. Differential loading, and diversity in the optical properties of the dyes, likely contributed to differences in labeling intensity. In the case of calcium green-2, it is not surprising that the labeling at resting calcium levels was not very bright, as this dye is very dim at zero Ca concentrations and increases fluorescence upon binding calcium. The other dyes were excited at wavelengths for which the fluorescence intensity was maximal at zero Ca and decreased upon binding calcium. Consequently, when calcium green-2 was used, it was more difficult to visualize the labeled structures, place the stimulus electrode, and choose the best recording site.

Measuring fluorescence levels

Experiments commenced several hours after loading, once fluorescence levels had stabilized. Parallel fiber tracts were stimulated extracellularly with an electrode (10–15 μm in diameter filled with extracellular solution) placed in the molecular layer near the fill site. Fluorescence changes were measured from a 150-μm-diameter spot situated 400–700 μm away from the stimulus site. The microscope was a Zeiss Axioskop FS, which had been mounted on an X/Y stage to allow movement of the field of view without disturbing the stimulus and recording electrodes.

The lamp housing with a quartz collector lens and power supply were made by Optiquip (model 1600 power supply), and a 150-watt Xenon bulb (Osram, Germany; 150 W/CR) was used. Illumination was gated with a TTL pulse and an electromechanical shutter (Vincent Associates, Rochester, NY). A Zeiss fluorescein filter set (450–490 nm excitation, an FT510 dichroic, and an LP 520 emission filter) was used for measurements with calcium green-2 and BTC. The filter set used with furaptra and Fura-2 was 380 HT 15 excitation (or 340 HT 15 for some Fura-2 measurements as indicated), a 430DCLP02 dichroic, and a 510WB40 emission filter (Omega Optical, Brattleboro, VT). The area of illumination was defined by an iris diaphragm. The collected light was focused onto a photodiode (Hamamatsu S1227–33BR) by a lens located in the image plane. Current to voltage conversion was accomplished with an operational amplifier (Burr Brown OPA111) and a 5 GΩ feedback resistor (Victoreen, Cleveland, OH). The output of the photodiode was filtered at 500 Hz with a 4-pole Bessel filter (Warner, Hamden, CT) and digitally recorded with a 16-bit converter (Instrutech, Great Neck, NY) with pulse control software (Herrington and Bookman, 1994). All experiments were done at 20–23°C.

When background fluorescence in an unlabeled region of the slice was greater than 5% of the fluorescence of the indicator, traces were corrected for background fluorescence. $\Delta F/F$ values were computed by 1), collecting a trace in which fibers were not stimulated; 2), collecting the stimulus trace; 3), scaling and subtracting the no stimulus trace from the stimulus trace; and 4), dividing by the fluorescence intensity and multiplying by 100, or −100 for BTC, furaptra, and Fura-2 in Figs. 4–10.

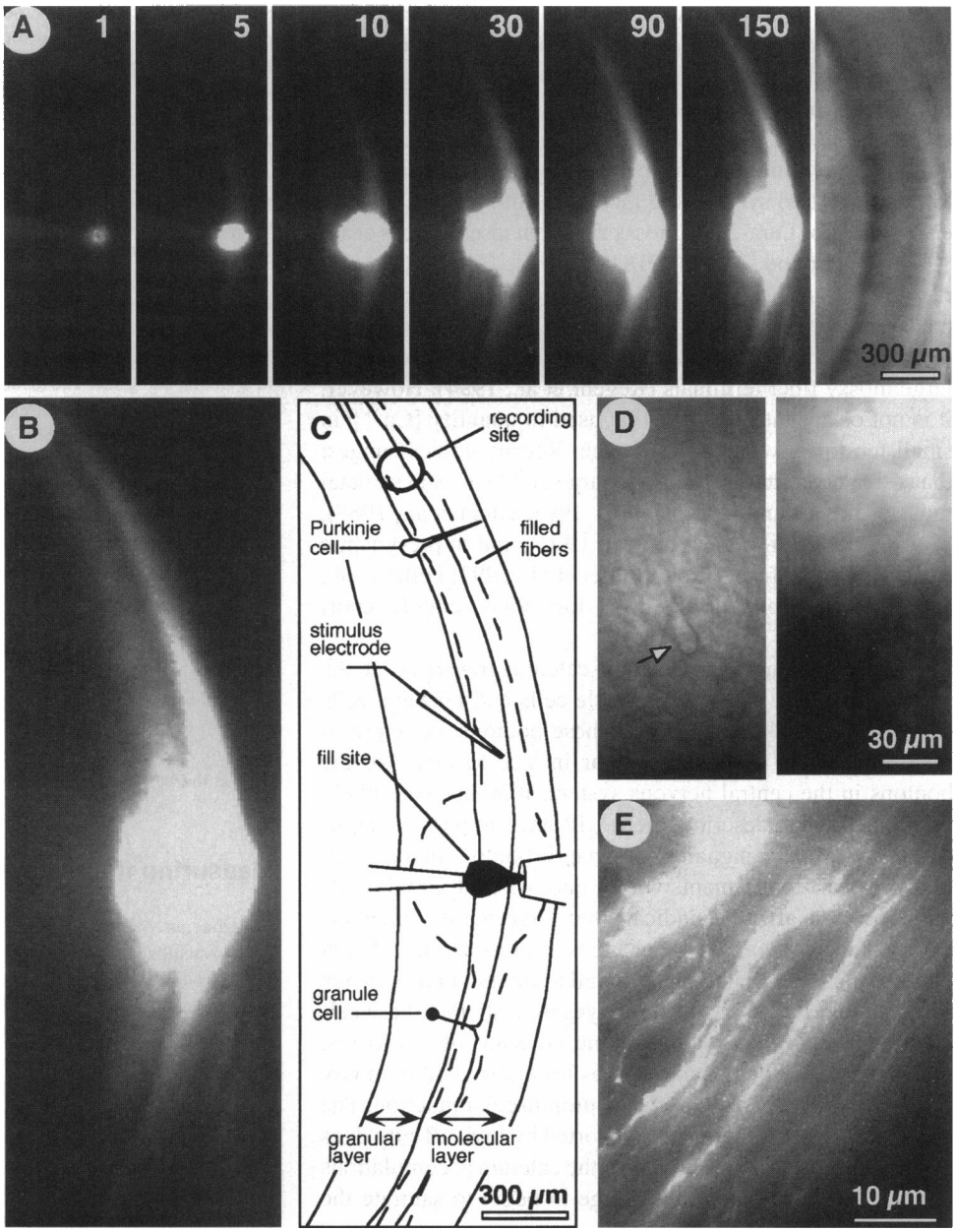

FIGURE 1 Labeling parallel fibers with calcium-sensitive fluorophores. (*A*) Furaptra fluorescence during and after labeling of a region in the molecular layer from time 0 to 30 min. Time of image acquisition relative to commencement of loading is indicated in minutes. Far right panel is a bright field image of the slice. (*B*) A higher magnification image of the fluorescence labeling observed in *A* 2.5 h after the start of labeling. (*C*) Schematic showing the layers of the cerebellum, the typical positions of the Purkinje and granule cells, and the arrangement of stimulus electrode and recording sites. (*D*) Bright field (*left*) and fluorescence (*right*) images of the labeling observed in another slice. Purkinje cells away from the fill site, such as the one indicated by the arrow, are clearly not labeled. (*E*) A high magnification view of the molecular layer reveals that parallel fibers and their associated terminals are labeled but that the cell bodies of neurons in the molecular layer are not. *A-C* and *E* are from experiment wa042794b; *D* is from experiment wa050494.

Fluorescence images

The fluorescence images of Fig. 1 were acquired with a cooled, charge-coupled device camera (Photometrics, Tucson, AZ). Low power images were obtained with a 5× objective and a 0.55× projection lens. High power images were obtained with either a 40× or 63× objective and an optivar.

Modeling the fluorescence response of different indicators

Numerical simulations of the fluorescence changes of indicators were performed on a microcomputer. A single compartment was used, and the following differential equation describing the reaction of the indicator with calcium was integrated by the Euler integration method:

$$\frac{d[\text{CaFluor}]}{dt} = k^+[\text{Fluor}][\text{Ca}] - k^-[\text{CaFluor}] \quad (1)$$

where [Fluor] is the concentration of unbound indicator, [Ca] is the free calcium concentration, [CaFluor] is the concentration of calcium bound to indicator, and k^+ and k^- are the on and off rates of the dyes. It was assumed that fluorophores were present in sufficiently low concentrations that they did not alter the calcium dynamics. Each stimulus increased free calcium by 300 nM, which then decayed to resting levels with a time constant of 150 ms. Resting calcium was 50 nM. The on rate for the simulations of Figs. 11, 13, and 14 was taken to be 2.5×10^8 M^{-1} s^{-1}, which is in the range reported for Fura-2 and furaptra (Table 1). The dissociation constants and reverse rate constants were chosen to match the properties of Fura-2 (K_d = 200 nM; k^- = 50 s^{-1}), calcium green-2 (K_d = 600 nM; k^- = 150 s^{-1}), and the low affinity dyes BTC and furaptra (K_d = 20 μM; k^- = 5000 s^{-1}). The simulations are meant to provide insight into the distortion of the calcium signals recorded with dyes that differ in their kinetic and equilibrium properties. No effort was made to simulate the absolute changes in fluorescence (ΔF/F) per action potential for each of the indicators; for all simulations the fluorescence intensity of the bound form of the indicator was taken to be 10 times that of the free form of the dye. Although differences in the

diffusion rates of indicators can significantly affect the fluorescence signals under some circumstances (Winslow et al. 1994; Nowycky and Pinter, 1993), because of the small size of parallel fiber presynaptic terminals, such considerations are unlikely to affect the fluorescence signals recorded here. For this reason we did not consider effects of differences in the diffusion coefficients of the indicators.

RESULTS

Detection of calcium transients in parallel fibers

Parallel fibers were filled with fluorescent indicators by locally applying a stream of the membrane-permeant form of the dye to a small region of the slice, as shown in Fig. 1. In the coronal slices of the cerebellum used for this study, the granule cells send their axons from the granular layer to the molecular layer, where they bifurcate and extend for several millimeters in either direction parallel to the surface of the slice (Fig. 1 *C*). Here they form *en passant* synapses, principally with Purkinje cells (Hamori and Szentagothai, 1964; Palkovits et al., 1971). The time series of Fig. 1 *A* shows the labeling produced by a continuous stream of dye applied to the molecular layer. The pipette used to deliver the dye was placed before the first image in the series and was removed after the fourth. Although in the immediate vicinity of the pipette tip many structures are labeled, in the molecular layer away from the fill site the only structures that were found to contain dye were the parallel fibers, as shown in Fig. 1 *E*. It appears that dye diffuses within the parallel fibers, labels a band in the molecular layer, and retrogradely fills scattered granule cells in the granular layer (Fig. 1, *B* and *D*). Purkinje cells and other cell types away from the fill site are not loaded (Fig. 1, *D* and *E*). BTC, Fura-2, and calcium green-2 showed a similar pattern of labeling to that of furaptra (see Materials and Methods).

An experiment arranged as in Fig. 1 *C*, in which parallel fibers were stimulated extracellularly and fluorescence transients were recorded optically from a location well away from the fill site, is shown in Fig. 2. A single extracellular stimulus of the parallel fibers increased the fluorescence for 340-nm illumination and decreased the fluorescence for 380-nm illumination, consistent with an increase in calcium. The changes in Fura-2 fluorescence were large, as much as 30% for single action potentials, which suggests that calcium increases were also large. In Fig. 2 *C*, and throughout the paper, changes in fluorescence are presented as ΔF/F signals that have been corrected for dye bleaching and background fluorescence, as described in Materials and Methods.

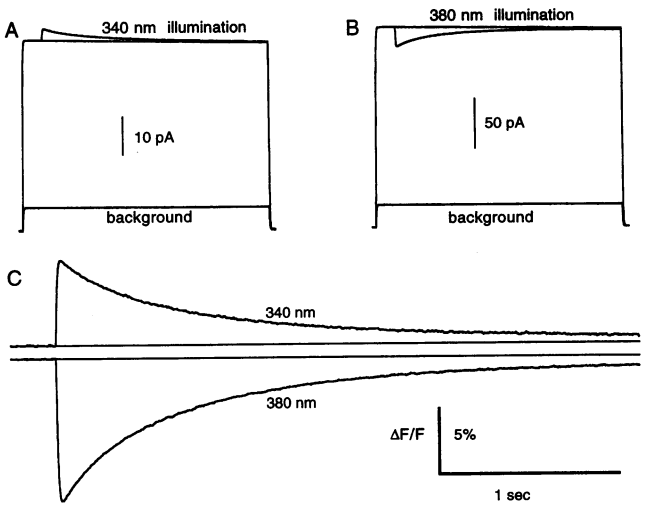

FIGURE 2 Optical signals recorded from labeled parallel fibers in response to a single stimulus. Background fluorescence and fluorescence of Fura-2-labeled parallel fibers (plus background) with and without a single stimulus for (*A*) 340 nm and (*B*) 380 nm illumination. (*C*) ΔF/F transients calculated by the procedure described in Materials and Methods.

Conventional ratiometric methods cannot be used to determine absolute calcium changes in parallel fiber nerve terminals

For these experiments it is not possible to quantify changes in free calcium ($[Ca^{2+}]$) with the following equation (Grynkiewicz et al., 1985), which is widely used to relate the Fura-2 fluorescence ratio to calcium concentration:

$$[Ca^{2+}] = K_d\left(\frac{R - R_{min}}{R_{max} - R}\right)\left(\frac{S_{f2}}{S_{b2}}\right), \quad (2)$$

where R_{min}, R_{max}, and S_{f2}/S_{b2} are constants defined according to Grynkiewicz et al. (1985), K_d is the dissociation constant of Fura-2, and R is the ratio of fluorescence for 340-nm to 380-nm illumination. For this equation to apply, the entire fluorescence used to determine R must come from regions at the same calcium concentration. This condition is clearly not satisfied in these experiments, in which stimulated and nonstimulated axons and terminals all contribute to the fluorescence signal, and there is no unique relation between ratio and calcium concentration. For example, a given ratio change could arise from a large calcium increase in a few terminals and no increase in the others or from a small increase in all of the terminals.

TABLE 1 Calcium-binding properties of the indicators

Indicator	Dissociation constant, K_d (μM)	Forward rate constant, k^+ ($M^{-1}s^{-1}$)	Reverse rate constant, k^- (s^{-1})	References
Fura-2	0.16	6.0×10^8	97	Kao and Tsien (1988)
	0.68	0.25×10^8	17	Hollingworth et al. (1992)
Calcium green-2	0.57			Molecular Probes data sheet MP3010
Furaptra	47	1.25×10^8	5875	Konishi and Berlin (1993)
BTC	7–14			Iatridou et al. (1994)

These properties were obtained from the indicated references.

The inapplicability of the ratio method is illustrated by Fig. 3. Fura-2 fluorescence was measured for 1 to 4 pulses with 340-nm and 380-nm illumination, and the ratio was determined. If Eq. 2 were used to convert the ratios in Fig. 3, *Ab* and *Bb*, to calcium, this would lead to the erroneous conclusion that the larger intensity stimuli produced larger calcium increases in the parallel fibers. A more likely interpretation of these findings is that elevating the stimulus intensity increases the number of fibers stimulated, without affecting the magnitude of calcium transients in the activated terminals.

Properties of fluorescence transients depend upon the fluorophore used

In Fig. 3, the changes in fluorescence and ratio were progressively smaller with each successive stimulus in a 20-Hz train. This was true for both weak and strong stimuli. The observed attenuation could result from less calcium entering the cell with each successive action potential or from calcium increases so large that they begin to saturate the Fura-2 response. To distinguish between these two possibilities, we used a number of calcium-sensitive fluorophores to measure calcium transients in parallel fiber nerve terminals.

The indicators used in this study differ in a number of properties (as summarized in Table 1), most notably in their dissociation constants, K_d, and their off rates, k^-, as defined by the reaction below:

$$\mathrm{Ca} + \mathrm{F} \underset{k^-}{\overset{k^+}{\rightleftarrows}} \mathrm{CaF}, \qquad (3)$$

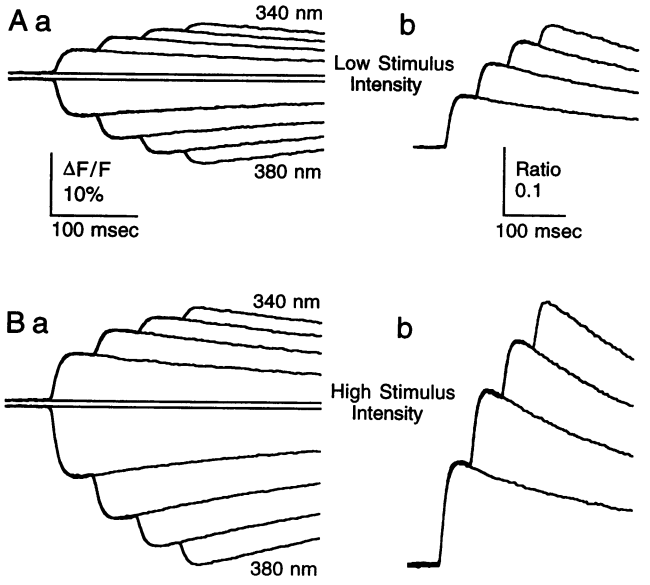

FIGURE 3 Changes in fluorescence and ratio (340-nm/380-nm-induced fluorescence) for Fura-2-labeled parallel fibers stimulated with brief trains. Superimposed changes in Fura-2 (*a*) fluorescence and (*b*) ratio in response to 20-Hz trains of one to four stimuli for (*A*) low intensity and (*B*) high intensity extracellular stimulation. The resting ratio was 0.81.

where F is the fluorophore, k^+ is the on rate, and $K_d = k^-/k^+$. The fluorescence transients observed with various indicators differed greatly. As shown in Fig. 4, for the relatively high affinity indicators Fura-2 and calcium green-2, the fluorescence change per spike decreased during the stimulus train. In contrast, for the low affinity indicators BTC and furaptra, each stimulus in a train produced approximately the same change in fluorescence.

For the excitation wavelengths used in Figs. 4–10, increases in calcium correspond to decreases in fluorescence for BTC (470-nm excitation), furaptra (380-nm excitation), and Fura-2 (380-nm excitation). To facilitate comparison, all fluorescence changes in Figs. 4–10 are presented as positive values.

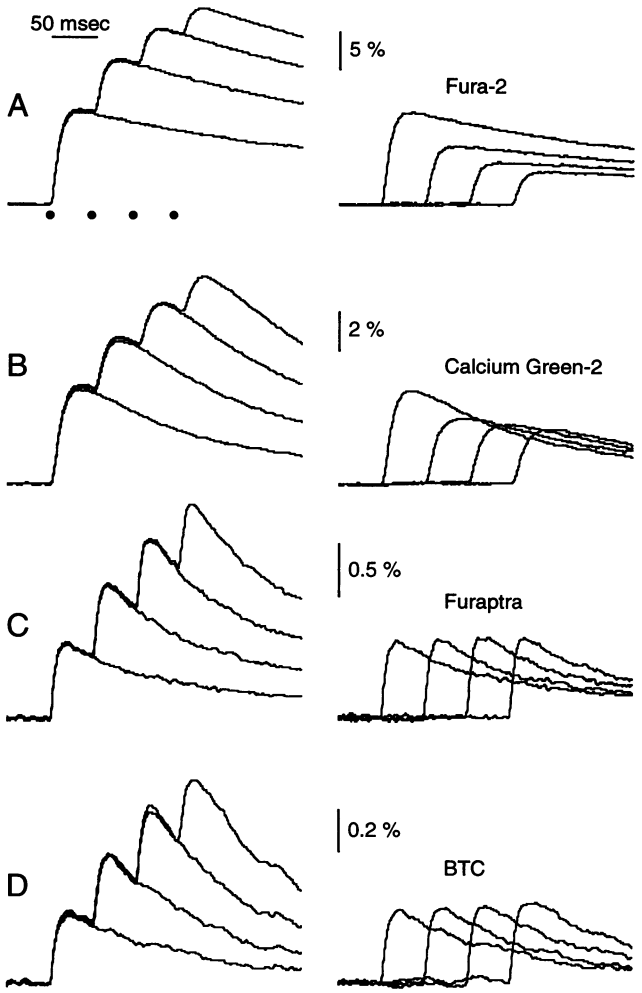

FIGURE 4 The properties of fluorescence transients evoked by short trains of action potentials depend on the calcium-sensitive fluorophore used. Parallel fibers were loaded with different calcium indicators and stimulated with 20-Hz trains consisting of one to four action potentials. The resulting fluorescence transients are shown for (*A*) Fura-2, (*B*) calcium green-2, (*C*) furaptra, and (*D*) BTC. The right panel of each set of fluorescence transients are the increases produced by each stimulus in the train. These were determined by subtracting the ΔF/F signal produced by a train of n stimuli from that obtained from a train of n + 1 stimuli. The timing of the stimulus pulses is shown in *A*.

These experimental findings shown in Fig. 4 suggested that Fura-2 does not faithfully report the calcium transient in parallel fiber nerve terminals. Using a variety of dyes to characterize the calcium transients appeared to hold promise, but before continuing these studies we decided to perform a number of experiments to test the nature of the fluorescence signals. Specifically, we wanted to determine whether they were produced by action potentials invading presynaptic terminals to trigger calcium entry through voltage-gated calcium channels.

Dye signals are caused by calcium influx into presynaptic structures

Fluorescence transients were almost completely eliminated in the presence of TTX, as shown in Fig. 5, indicating that depolarization provided by Na action potentials is required to trigger calcium influx. However, when the stimulus electrode was placed within several hundred microns of the recording site, and exceptionally large stimulus currents were used, the fluorescence transients were not completely eliminated by TTX but could be eliminated by the potent calcium channel antagonist Cd (not shown). This suggested that it was possible to directly depolarize parallel fibers and open calcium channels by using stimulus conditions much more extreme than those used in this study. We also found (not shown) that 6-cyano-7-nitroquinoxaline-2,3-dione (CNQX; Honore et al., 1988), which eliminates the excitatory synaptic inputs to cerebellar Purkinje cells, did not affect the $\Delta F/F$ signals; this indicates that calcium influx into postsynaptic cells does not contribute to the fluorescence signal.

Cd greatly reduced the fluorescence transients of all dyes, suggesting that the fluorescence transients arise from calcium influx through voltage-gated calcium channels. Cd rapidly reduced the fluorescence transients of Fura-2 (Fig. 6 *A*) and calcium green-2 (Fig. 6 *B*). This rapid reduction was accompanied by a change in the fluorescence intensity that became more pronounced while Cd was applied and persisted during washout. It is likely that Cd reduces $\Delta F/F$ primarily by blocking calcium entry, as the abrupt decrease in $\Delta F/F$ signals occurs before changes in fluorescence intensity are appreciable. It is not possible to quantitate the reduction of $\Delta F/F$ by Cd for these dyes, as secondary effects that alter absolute fluorescence also seem to decrease $\Delta F/F$ signals and prevent recovery of $\Delta F/F$ upon washout. It appears that Cd entered the presynaptic terminals, where it bound to the indicator, thereby changing its fluorescence and the $\Delta F/F$ signals. Such interactions of Cd with Ca-sensitive fluorophores have been documented (Hinkle et al., 1992). Interestingly, Cd did not appreciably alter the absolute fluorescence of furaptra (Fig. 6 *C*, for concentrations of 100 μM and below), and its reduction of furaptra fluorescence transients was reversible. This indicates that Cd entry into the parallel fibers does not compromise the measurement of calcium with furaptra (although for much higher Cd concentrations this possibility cannot be excluded).

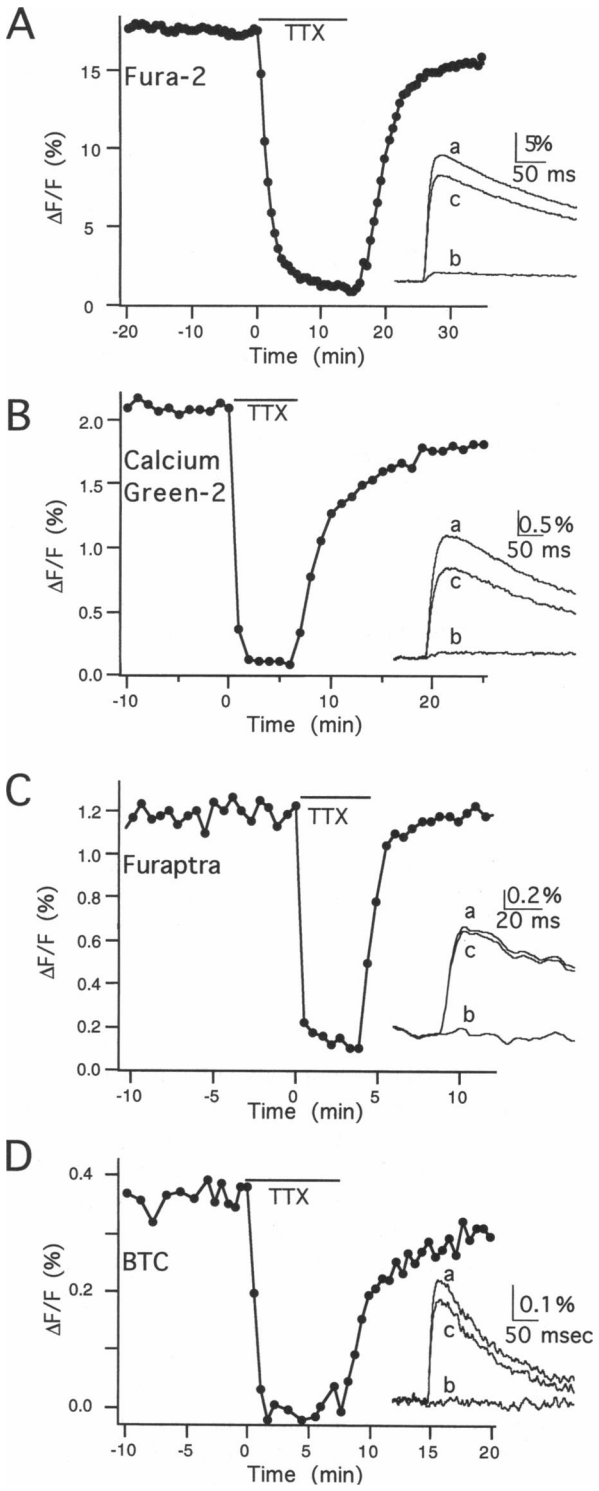

FIGURE 5 Fluorescence transients are eliminated by TTX. The effect of 400 nM TTX on the fluorescence transients evoked by a single stimulation of the parallel fibers is shown for (*A*) Fura-2, (*B*) calcium green-2, (*C*) furaptra, and (*D*) BTC. Inset traces were obtained (*a*) before TTX application, (*b*) after the block of TTX had plateaued, and (*c*) after washout of TTX.

Additional experiments were performed to examine the sources of calcium that give rise to the stimulus-evoked fluorescence transients. We will summarize these results, which

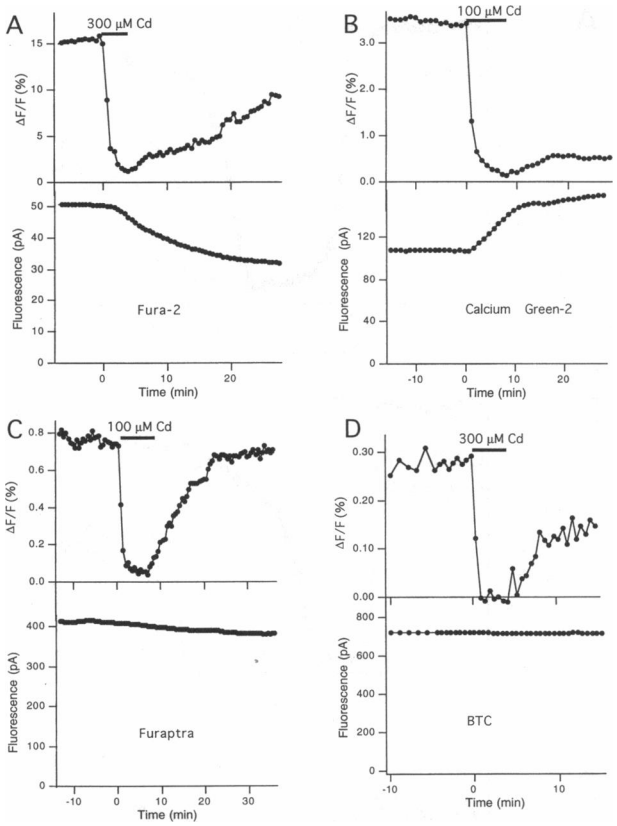

FIGURE 6 The effect of Cd on fluorescence transients evoked by a single stimulation (*upper graphs*) and absolute fluorescence intensity (*lower graphs*). (*A*) Fura-2, (*B*) calcium green-2, (*C*) furaptra, and (*D*) BTC.

cannot be included because of lack of space. First, release from internal stores does not appear to contribute to calcium transients in parallel fiber terminals, as the amplitude of these transients remains unaffected by agents that affect internal stores such as thapsigargin (Thastrup et al., 1990) and ryanodine (Anderson et al., 1989). Second, the reduction of furaptra fluorescence transients by Cd was well approximated by 1:1 binding with a dissociation constant of approximately 6 μM (Mintz, Sabatini, and Regehr, submitted for publication). This supports the view that the fluorescence transients we detect are produced by influx through voltage-gated calcium channels. Third, the calcium transients are reduced by approximately 90% by a coapplication of the calcium channel toxins ω-conotoxin-GVIA (Fujita et al., 1993; Williams et al., 1992), ω-Aga-IVA (Mintz et al., 1992), and ω-conotoxin MVII-C (Hillyard et al., 1992). It is likely that the fluorescence changes observed in these experiments are caused primarily by calcium transients in presynaptic terminals and not in the axons. It is estimated that for parallel fibers the volume of the boutons is approximately three times as large as the volume of the axons (Palay and Chan-Palay, 1974). In addition, it is likely that calcium channels are present at a much higher density in presynaptic terminals near release sites than in the axon, as has been shown for a number of other synapses (Delaney et al., 1989; Robitaille et al., 1990; Smith et al., 1993).

Time course of fluorescence transients

Once it was established that the fluorescence transients were produced by calcium influx into presynaptic structures through voltage-gated calcium channels, we returned to the examination of calcium dynamics with the dyes. The first question to answer was whether the fluorophores accurately reported the time course of calcium transients. As shown in Fig. 7, the fluorescence change produced by a single stimulus decayed more rapidly for BTC and furaptra than for Fura-2 and calcium green-2. The most likely interpretation of this observation is that the high affinity indicators Fura-2 and calcium green-2 do not follow the rapid calcium changes because they are slow and their response to calcium saturates, whereas furaptra and BTC, which have much lower affinities and faster kinetics, faithfully report the calcium transient. This issue is dealt with further in Fig. 11 and the accompanying text.

Amplitudes of fluorescence changes evoked by multiple action potentials measured with different dyes

To test the relationship between the amplitudes of calcium transients and fluorescence changes, we measured fluorescence transients produced by 100-Hz trains of 1 to 10 action potentials, as shown in Fig. 8. These trains had the advantage that the interstimulus interval was short enough that calcium in the terminals had very little chance to decay between stimulus pulses, allowing calcium to accumulate to relatively high levels within the terminals. As in Fig. 4, the fluorescence changes per spike decreased markedly during the train for Fura-2 and calcium green-2 but not for furaptra and BTC. This is shown for representative experiments in Fig. 8, *A-D*, and is summarized for a number of experiments in Fig. 8, *E* and *F*.

The most straightforward interpretation of these findings is that each stimulus in a train produces the same increase

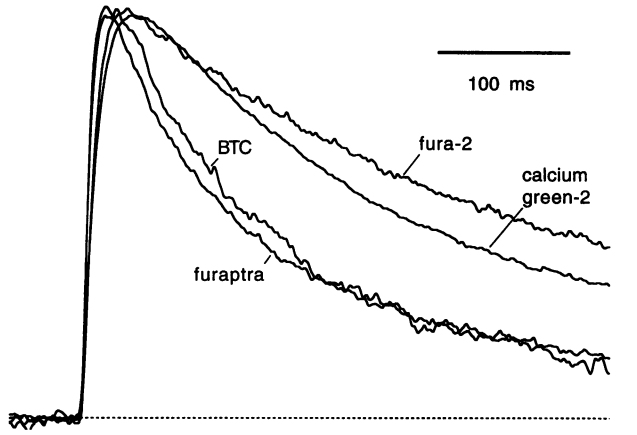

FIGURE 7 Time course of ΔF/F transients produced by single stimuli for different calcium indicators. Traces have been normalized to facilitate comparison.

in free calcium in parallel fibers, as reported by BTC and furaptra. But these calcium increases are sufficiently large to begin to saturate the responses of Fura-2 and calcium green-2; consequently, for these dyes $\Delta F/F$ is not linearly related to changes in $[Ca^{2+}]_i$.

Fura-2 fluorescence transients depend upon the loading time and the external calcium concentration

In addition to inaccurately reporting calcium changes, as in Figs. 4, 7, and 8, Fura-2 can affect the calcium transients. Fluorescence transients in parallel fibers labeled for 5–10 min were compared with those labeled for 30 min. We attempted to minimize other potential sources of variation by loading parallel fiber tracts in the same slice with the same loading electrode and with the same pressure. The decay time was slowed significantly in experiments in which the terminals had been loaded for 30 min (Fig. 9, *A-C*). In the fiber tract filled for the shorter amount of time, during a 100-Hz train there was more saturation in peak fluorescence changes (Fig. 9 *D*), and the fluorescence change per pulse decreased more rapidly (Fig. 9 *E*).

These findings suggest that the longer loading times introduce into the terminals quantities of Fura-2 that have a buffer capacity comparable with that of endogenous buffers. As shown by a number of recent studies (Delaney and Tank, 1994; Swandulla et al., 1991; Regehr et al., 1994; Neher and Augustine, 1992; Regehr and Tank, 1992; Sala and Hernandez, 1990; Tank et al., 1991), Fura-2 can increase the buffer capacity of cells, thereby slowing the time constant of calcium decay and decreasing the amplitude of calcium transients. Increasing the buffer capacity, while keeping calcium influx constant, leads to a smaller increase in free calcium per stimulus and less saturation of Fura-2. The lower affinity buffers, such as BTC and furaptra, are unlikely to produce this sort of distortion, as for a given buffer concentration the buffer capacity is inversely proportional to the dissociation constant, for $[Ca^{2+}]_i \ll K_d$ of the buffer. Not surprisingly, we found no difference between the fluorescence transients of furaptra-filled terminals labeled for 5 min or for 30 min (not shown).

From experiments with multiple types of dyes, such as those in Fig. 8, it was clear that fura-2 did not accurately report the calcium transients in parallel fiber nerve terminals. However, using the knowledge that the calcium influx per spike appeared to be constant, we sought to test whether the degree of saturation of the Fura-2 response could be used to quantify changes in $[Ca^{2+}]_i$. The calcium influx per stimulus was altered by changing external calcium levels. As shown in Fig. 10, for 100-Hz stimulation, the fluorescence saturation became less pronounced as the external calcium was decreased. However, even when external calcium levels were reduced to 0.25 mM Ca, $\Delta F/F$ showed appreciable saturation.

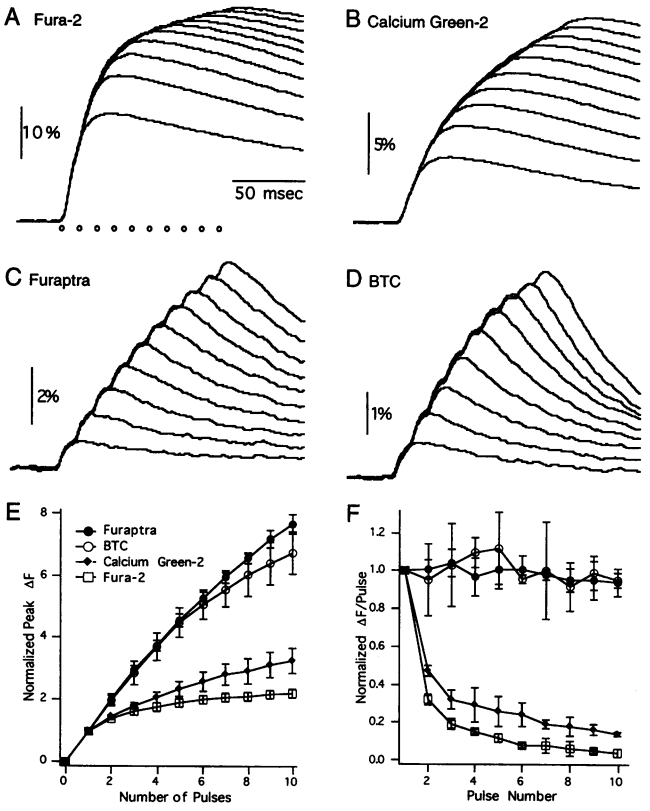

FIGURE 8 Fluorescence transients produced by high frequency stimulation differ greatly for various indicators. $\Delta F/F$ changes evoked by 100-Hz trains of 1 to 10 stimuli for (*A*) Fura-2, (*B*) calcium green-2, (*C*) furaptra, and (*D*) BTC. (*E*) Comparison of the buildup of fluorescence signals and (*F*) the $\Delta F/F$ signal per stimulus. Points in *E* and *F* are averages normalized to the change evoked by the first stimulus in the train. Error bars are standard deviations for experiments performed in three slices (Fura-2), four slices (calcium green-2), six slices (furaptra), and five slices (BTC).

Simulations of calcium transients in parallel fibers

Simulations were performed to determine whether the fluorescence transients observed with the different dyes were consistent with the reported properties of the fluorophores used in the study. An additional goal of this section was to quantify changes in $[Ca^{2+}]_i$.

These single-compartment simulations ignored spatial gradients, which are expected to collapse rapidly within the small confines of a parallel fiber bouton. We estimate the characteristic time to be approximately $r^2/6D = 4$ ms (Crank, 1975), with $D = 10^{-7}$ cm^2/s as the effective diffusion coefficient of calcium, and $r = 0.5$ μm as the radius of the terminal. It was assumed that the amount of dye introduced into the terminals did not influence the time course of the transients. On the basis of the data obtained with BTC and furaptra, we assumed that each stimulus in a train increased the free calcium levels in the terminal by a constant amount and that calcium decayed to resting levels with a time constant of 150 msec. The resting calcium levels were assumed to be 50 nM.

Simulations of fluorescence transients produced by single stimuli, shown in Fig. 11 for fluorophores with

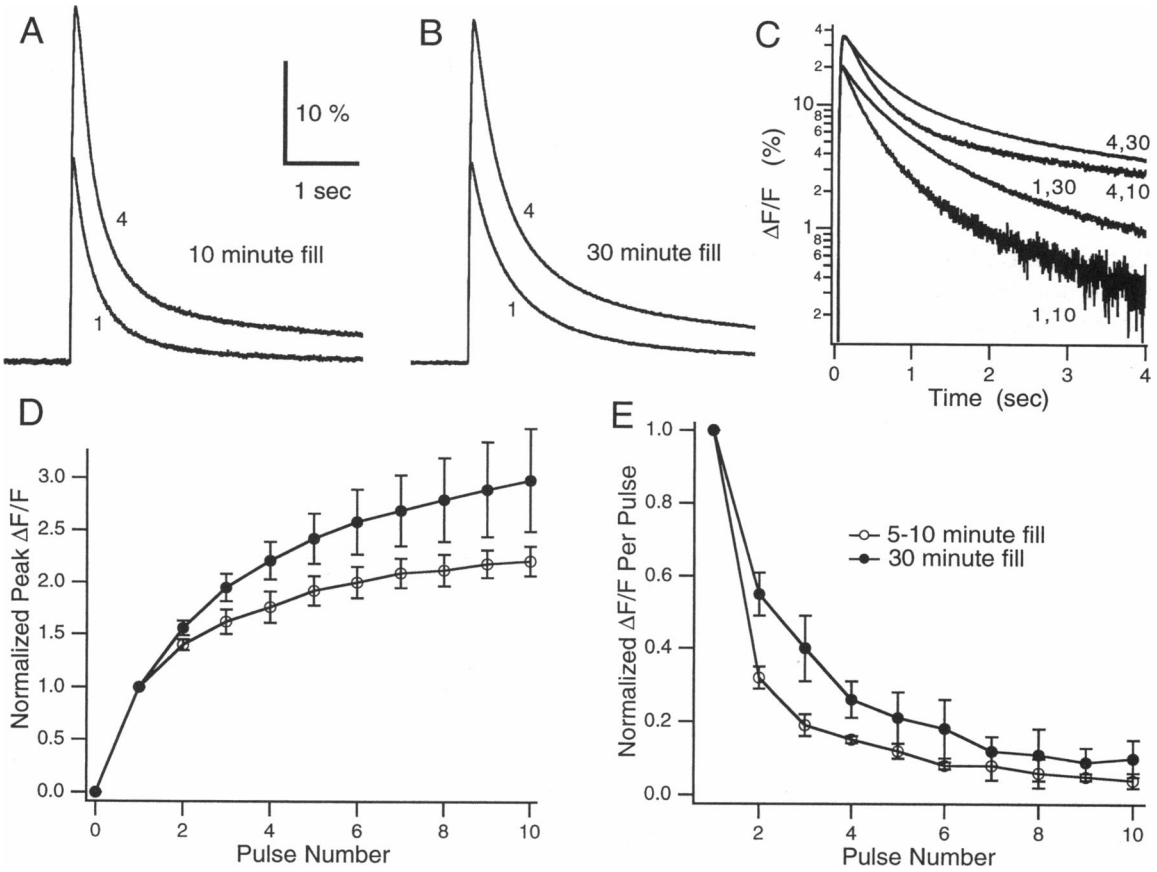

FIGURE 9 Labeling time influences the properties of Fura-2 transients. Fluorescence changes for one and four stimuli at 100 Hz for parallel fiber tracts labeled for (*A*) 10 min and (*B*) 30 min. (*C*) A semilog plot of the traces in *A* and *B* for comparison of the time course of calcium decay. Labels refer to the number of stimuli and the loading time. (*D*) Comparison of the buildup of fluorescence signals and the (*E*) ΔF/F signal per stimulus, normalized to the response to the first stimulus, for 100-Hz stimulus trains. Points in *D* and *E* are averages with standard deviations for experiments performed in three slices (5–10 min labeling) and five slices (30 min labeling).

properties similar to those used in this study, indicate that high affinity dyes are incapable of accurately reporting large and rapid calcium changes. Part of the distortion is a result of the slow kinetics of these dyes. As shown in Fig. 11 *A*, for a small calcium increase there is a delay in the time to peak for the high affinity dyes. This is expected, as for a step increase of calcium from 0 to $[Ca^{2+}]_i$ the concentration of the indicator bound to calcium should increase with a time constant $\tau = (k^+[Ca^{2+}]_i + k^-)^{-1}$ (Regehr et al., 1994). In addition, the decay time is prolonged for dyes with slow kinetics, although, as shown in Fig. 11 *A*, the effect of the slow off rate does not greatly affect the time course of calcium decay. Considering calcium returning instantaneously from elevated levels to 0 provides a quantitative estimate of the effect of off rate on fluorescence decay. In this case the calcium dissociates from the indicator with a time constant of $\tau = 1/k^-$, which for Fura-2 is 1/50 s^{-1} = 20 ms, for calcium green-2 is approximately 1/150 s^{-1} = 6.7 ms, and for BTC and furaptra is approximately 1/5000 s^{-1} = 0.2 ms; these time constants are all much faster than the estimated decay time of calcium (τ = 150 ms). The off rates used here for calcium green-2 and BTC are estimates made on the basis of reported values for their dissociation constants and an on rate of 2.5 × 10^8 M^{-1} s^{-1}.

Another factor that contributes to the distortion is that the large calcium levels begin to saturate the response of the high affinity dyes. This is illustrated by comparing the time course of fluorescence signals for large (Fig. 11 *B*) and small (Fig. 11 *A*) calcium transients. The fluorescence decays more slowly for high affinity indicators when the calcium increases are large, as in Fig. 11 *B*. The simulations of Fig. 11 *B* are in good qualitative agreement with experimentally observed calcium transients for single stimuli shown in Fig. 7. For subsequent simulations a calcium increase per spike of 300 nM was used. This value was chosen to match the observed saturation of Fura-2 response.

Although an on rate of 2.5 × 10^8 M^{-1} s^{-1} was used for the simulations of Figs. 11, 13, and 14, we also examined the effect of changing the on and off rates while keeping the affinity constant (not shown). For simulations in which slower on rates were used, the fluorescence peaked much more slowly than the measured fluorescence transients. This suggests that the on rates for the indicators in parallel fiber terminals were similar to the diffusion limited values reported in vitro (see Table 1).

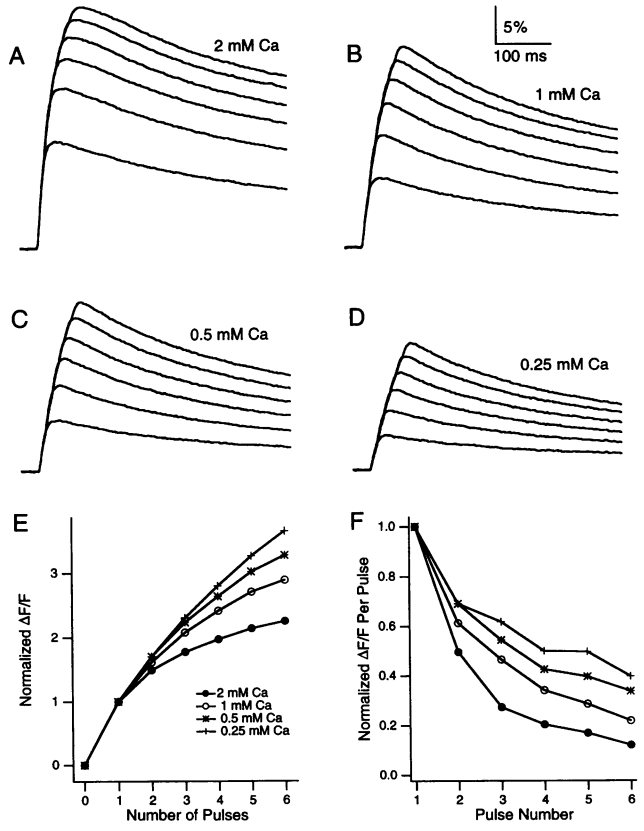

FIGURE 10 Dependence of Fura-2 fluorescence on extracellular calcium concentration. Fura-2 fluorescence was measured in the same preparation for 100-Hz trains of one to six stimuli in different external calcium concentrations: (*A*) 2 mM, (*B*) 1 mM, (*C*) 0.5 mM, and (*D*) 0.25 mM. (*E*) Comparison of the buildup of fluorescence signals and (*F*) the ΔF/F signal per stimulus, normalized to the response produced by the first stimulus. In these experiments the divalent concentration was kept constant by adjusting the Mg concentration. For these conditions the amplitude of the presynaptic volley measured extracellularly remained constant, indicating that the number of stimulated fibers remained constant for different concentrations of $[Ca^{2+}]_i$.

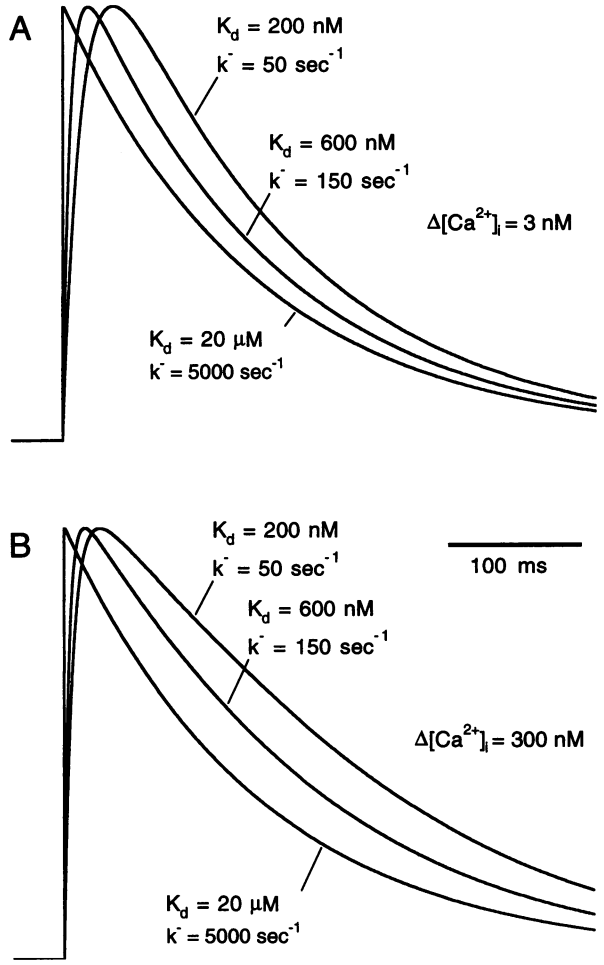

FIGURE 11 Simulations showing the fluorescence transients for dyes with the indicated dissociation constants and off rates for a calcium transient that rises abruptly from a resting level of 50 nM and decays to rest with a time constant of 150 ms. (*A*) Calcium increase of 3 nM per stimulus and (*B*) calcium increase of 300 nM per stimulus. Traces are normalized to facilitate comparison.

The calcium affinity of an indicator dictates the degree of saturation of its fluorescence response over a given range of calcium concentration. This is shown in the simulation of Fig. 12, in which the equilibrium relationship between calcium levels and fluorescence are shown for three dyes that differ only in their dissociation constants. In the range 0–3000 nM $[Ca^{2+}]_i$, the dye with the lowest affinity has an essentially linear relationship between calcium and fluorescence, but its fluorescence change is quite small. For the high affinity dye, the fluorescence change is larger, but the response of the dye begins to saturate. If the curves are normalized to the fluorescence level at 300 nM, as in Fig. 12 *B*, the saturation of the high affinity dyes is accentuated. The similarity of Fig. 12 *B* to Fig. 8 *E* suggests that the measured saturation of the response for calcium green-2 and Fura-2 can be accounted for by their high affinities. As this is an oversimplification that does not take into account the decay of calcium between stimuli and the kinetics of the indicators, more detailed simulations were performed.

A simulation of the fluorescence response for an experiment similar to that of Fig. 4 is shown in Fig. 13. The calcium transients produced by four 20-Hz trains consisting of one to four action potentials are shown in Fig. 13 *A*. To the right is the calcium increase produced by each additional pulse in the train. The response for a dye with a dissociation constant of 200 nM, shown in Fig. 13 *B*, saturates during the train, as was observed experimentally for Fura-2 (Fig. 4 *A*). The saturation is less apparent for a dye with a dissociation constant of 600 nM (Fig. 13 *C*), just as was observed experimentally for calcium green-2 (Fig. 4 *B*). Finally, the dye with a dissociation constant of 20 μM faithfully reported the time course of the calcium transients and did not appreciably saturate during the train (Fig. 13 *D*), as observed with BTC and furaptra (Fig. 4, *C* and *D*).

Simulations closely approximated the observed fluorescence transients for 100-Hz stimulus trains. The calcium transients used in these simulations are shown in Fig. 14 *A*. Simulations with a dissociation constant of 200 nM (Fig. 14

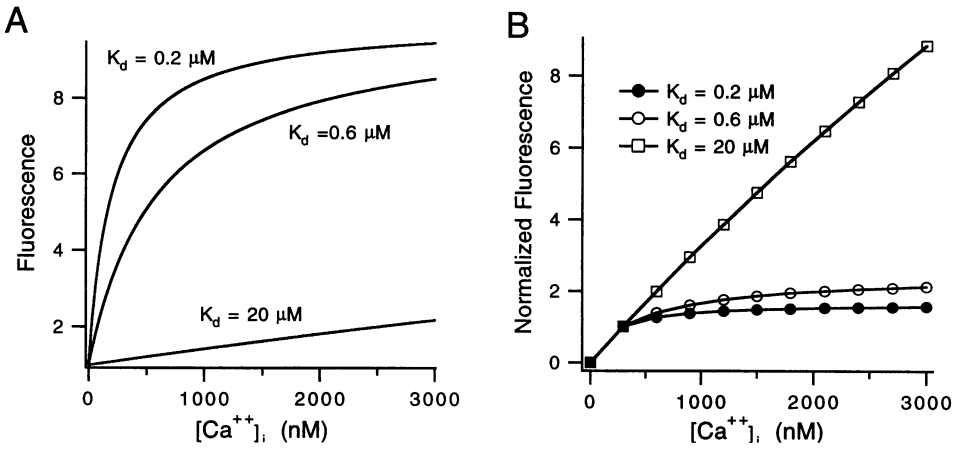

FIGURE 12 Saturation of fluorophores with different dissociation constants for calcium. (*A*) Fluorescence intensity in arbitrary units as a function of calcium concentration for equilibrium conditions in which the dyes differ only in their dissociation constants. (*B*) Fluorescence intensities of *A* normalized to the intensity at 300 nM calcium. Points correspond to increments in free calcium of 300 nM.

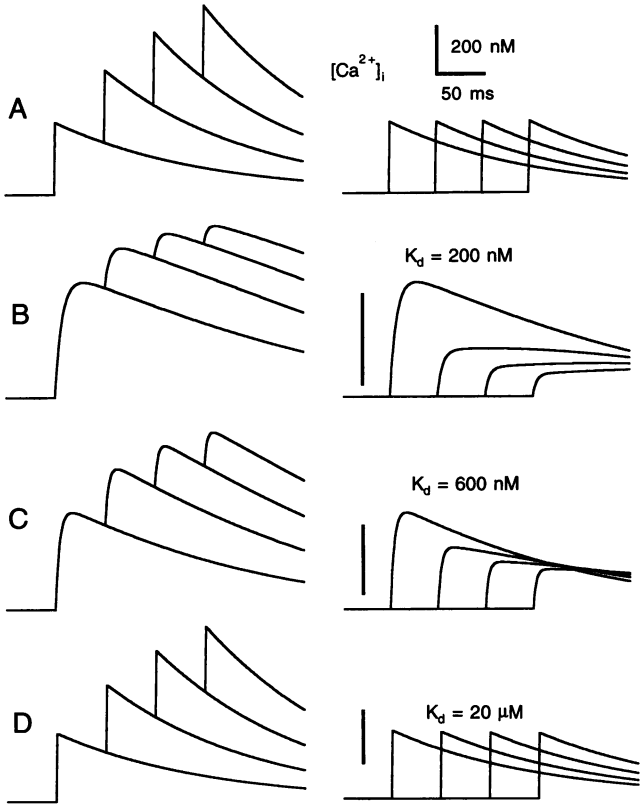

FIGURE 13 Simulations of fluorescence transients detected by different indicators for one to four stimuli delivered at 20 Hz. (*A*) Calcium signals used in the simulations. Calcium changes per stimulus are shown to the right. Simulated fluorescence transients are shown for dyes differing only in their off-rates (*B-D*). Fluorescence changes per stimulus are shown to the right. Scale bars correspond to (*B*) 100%, (*C*) 100%, and (*D*) 10% changes in ΔF/F.

B) showed approximately the same degree of saturation as Fura-2 fluorescence transients (Fig. 8 *A*). Those with a dissociation constant of 600 nM (Fig. 14 *C*) were similar to calcium green-2 fluorescence transients. When a dissociation constant of 20 μM was used (Fig. 14 *D*), the transients faithfully followed the calcium levels and were similar to fluorescence transients measured with BTC and furaptra (Fig. 8, *C* and *D*).

The degree of saturation and the fluorescence change per stimulus for these simulations (Fig. 14, *E* and *F*) were similar to those observed experimentally (Fig. 8, *E* and *F*). These curves can be used to estimate the magnitude of the increase in $[Ca^{2+}]$ (see Discussion).

DISCUSSION

Using multiple fluorescent calcium indicators and simulations of their fluorescence transients, we have found that calcium increases produced in parallel fiber terminals by single action potentials are exceptionally large and decay rapidly to resting levels. Below we 1), discuss the limitations and advantages of different indicators for the measurement of calcium transients in small presynaptic terminals typical of those in the mammalian brain; 2), compare the calcium transients in parallel fiber terminals with those in other presynaptic terminals; and 3), introduce a novel method for estimating the magnitudes of calcium changes in presynaptic terminals from the degree of saturation of high affinity indicators.

Limitations and advantages of different calcium indicators

In choosing a dye to detect calcium levels in presynaptic terminals there is a trade-off between sensitivity and linearity. There is no single dye that is best suited to measuring calcium levels in parallel fiber terminals in all circumstances.

It appears that high affinity dyes such as Fura-2 distort the measured calcium signals in several ways. Large increases in calcium saturate the responses of these dyes, as in Fig. 12. This accounts for the dramatic decrease in the ΔF/F per stimulus observed during a train when using high affinity

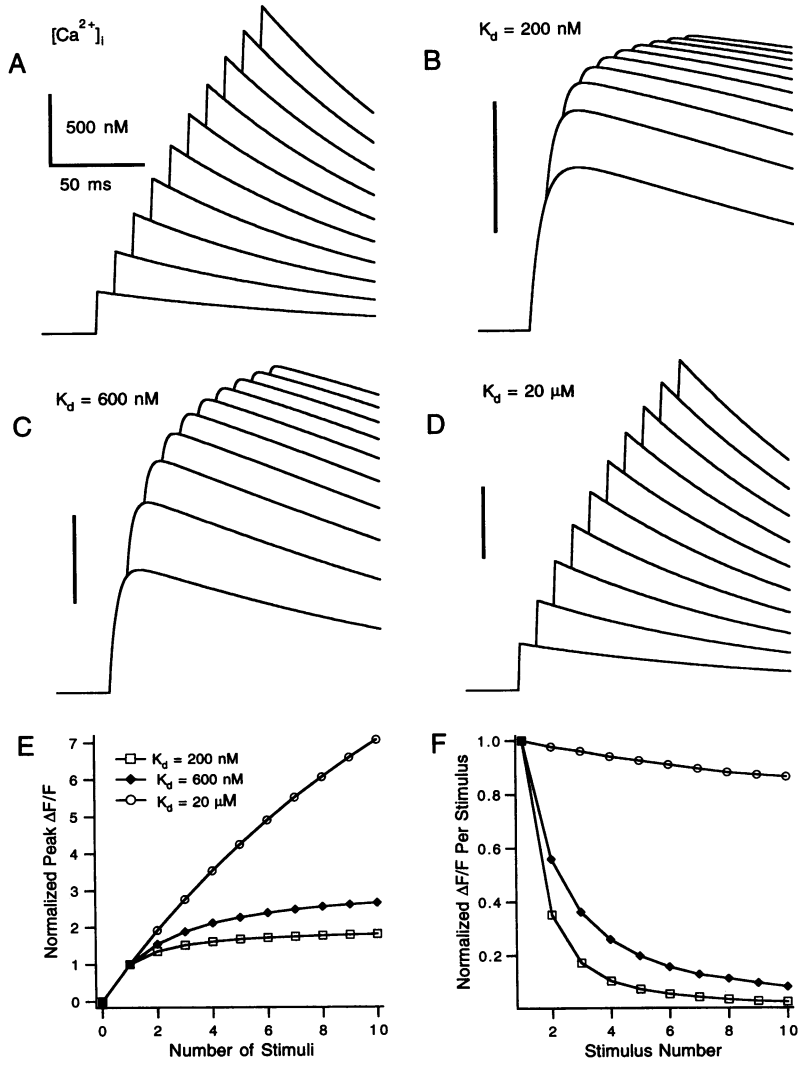

FIGURE 14 Simulations of fluorescence transients for different fluorophores for 100-Hz trains of 1 to 10 stimuli. (*A*) Calcium signals used in the simulation and (*B-D*) fluorescence transients for fluorophores with the indicated off rates. (*E*) Comparison of the buildup of fluorescence signals and (*F*) the ΔF/F signal per stimulus normalized to the response to the first stimulus. Scale bars correspond to (*B*) 100%, (*C*) 100%, and (*D*) 20% changes in ΔF/F.

dyes. In addition, the slow off rates of these dyes limit their response times. It may be generally true that high affinity indicators are unable to track presynaptic calcium transients in small terminals in the vertebrate brain. In presynaptic structures in the frog tectum, Fura-2 fluorescence changes begin to saturate during a stimulus train (Feller et al., 1993). We have also found this to be the case for terminals associated with CA3 pyramidal cells from the hippocampus (Regehr, unpublished observations). It appears that ratiometric measurements of calcium levels with Fura-2 in CA3 pyramidal cell terminals, as reported previously (Wu and Saggau, 1994a,b), were subject to errors in determining the amplitude and time course of calcium transients.

Low affinity indicators such as furaptra and BTC are well suited to measuring changes in calcium influx. For our experimental conditions, there is a linear relationship between the total number of calcium ions entering a terminal per stimulus, $\int I_{Ca}dt/2e$, and peak changes in $[Ca]_i$ or fluorescence:

$$\left(\frac{\Delta F}{F}\right)_{peak} \alpha\, \Delta[Ca^{2+}]_{peak} \alpha \int I_{Ca}dt\left(\frac{[B_{en}]}{K_{en}} + \frac{[B_{indicator}]}{K_{indicator}}\right)^{-1}, \quad (4)$$

where I_{Ca} is the calcium current for a terminal, e is the elementary charge, and $[B_{en}]$, K_{en}, $[B_{indicator}]$, and $K_{indicator}$ are, respectively, the concentration and dissociation constants of the endogenous calcium buffers and of the indicator (modified from Neher and Augustine, 1992, for $[Ca^{2+}]_i \ll K_{indicator}$ and $[Ca^{2+}]_i \ll K_{en}$). Equation 4 does not hold for high affinity indicators such as Fura-2 when calcium increases are large, as in parallel fiber terminals. Owing to the saturation of the Fura-2 response, there is a sublinear relationship between peak fluorescence changes and calcium increases for Fura-2.

Low affinity indicators are, however, not very well suited to measuring the small calcium levels that persist for tens of

seconds after a stimulus train. The small size of these signals presents a serious problem. If an increase in presynaptic calcium of 300 nM corresponds to a fluorescence change of 0.5% (a reasonable estimate for furaptra), then several seconds after a stimulus train, when the calcium has decayed to less than 10 nM above rest, the change in fluorescence would be less than 0.02%. Even small variations in the intensity of illumination or in the rate of bleaching can compromise the detection of such small calcium changes. In addition, for indicators such as furaptra, which are sensitive to magnesium as well as calcium, increases in magnesium could produce the smaller more persistent changes in fluorescence (Konishi and Berlin, 1993). Higher affinity indicators are much better suited to these sorts of measurements, as long as they are used with appropriate caution. Calcium must have decayed to levels at which there is roughly a linear relationship between changes in calcium and fluorescence changes; this must be verified by experiments such as those of Figs. 8 and 10. In addition, the rate of calcium decay must be slow compared with $(k^-)^{-1}$ of these indicators.

Buildup of calcium during stimulus trains

For the low affinity calcium indicators BTC and furaptra, each stimulus in a 100-Hz train of 10 pulses produces the same increase in fluorescence. The most straightforward interpretation of these findings is that for each stimulus in the train the calcium influx and the increase in free calcium both remain constant. This suggests that the dominant buffers in these terminals are low affinity, for, if they were high affinity, each successive stimulus in the train would produce successively larger increases in free calcium as the endogenous buffers became saturated. Calcium buffering must be dominated by endogenous calcium-binding proteins, because furaptra did not significantly alter the decay time of calcium (which should scale as the buffer capacity, see below). These considerations suggest that the dissociation constant of the endogenous buffer is much greater than the calcium levels reached during a 10-pulse train delivered at 100 Hz, which we estimate to be several micromolar.

Calcium indicators can influence presynaptic calcium transients

As shown for Fura-2 in Fig. 9, sufficient concentrations of a calcium indicator can be introduced by local perfusion of a membrane-permeant form to alter calcium transients in parallel fibers. Similar effects on calcium dynamics by the addition of calcium buffers have been reported in a number of other preparations and are expected from theoretical considerations (Neher and Augustine, 1992; Regehr and Tank, 1992; Sala and Hernandez, 1990; Tank et al., 1991). The most closely related experiments were performed at the crayfish neuromuscular junction (Tank et al., 1991). In that preparation, the time constant of decay is proportional to the total buffer capacity of the presynaptic terminal. If an exogenous buffer such as Fura-2 is introduced, the buffer capacity of the terminal is increased and calcium decays exponentially with a time constant, τ:

$$\tau \propto \left(\frac{[B_{en}]}{K_{en}} + \frac{[B_{indicator}]}{K_{indicator}}\right). \quad (5)$$

Introducing more Fura-2 into parallel fibers by loading for longer periods of time prolonged the decay time of fluorescence changes, indicating that the Fura-2 introduced into the parallel fibers had a buffer capacity comparable with that of the endogenous buffers (i.e. $[B_{indicator}]/K_{indicator}$ and $[B_{en}]/K_{en}$ are similar in size). In addition, with longer loading times saturation of the fluorescence changes during a high frequency train was less pronounced, consistent with elevated levels of Fura-2 reducing the peak change in free calcium per action potential (Fig. 9, Eq. 4).

Lower affinity buffers such as furaptra did not appear to have a significant effect on the time course of calcium decay, even if the loading times were quite long. This is not surprising, as the effect on the buffer capacity is inversely related to the dissociation constant of the buffer, and it would take approximately 100 times as much furaptra (20,000 nM/200 nM) to alter the buffer capacity of the terminal to the same degree as did Fura-2 when $[Ca^{2+}]_i \ll K_{indicator}$.

Another issue in selecting a calcium-sensitive dye is whether it can be used in the presence of divalents such as Cd. It appears that bath application of Cd can lead to a gradual buildup of Cd within cells, which interferes with the detection of calcium transients by dyes such as calcium green-2 and Fura-2 (Hinkle et al., 1992). Therefore, these dyes are poorly suited to quantifying the effect of Cd on calcium transients. Indicators such as furaptra are much less sensitive to the buildup of Cd within a cell and so are much better suited to measuring the effect of Cd on calcium transients.

Quantification of calcium accumulations in parallel fibers

As discussed in Results, the ratio method cannot be used to convert fluorescence transients to calcium transients for these experiments. However, we have been able to estimate the magnitude of calcium transients by using the saturation of the response of Fura-2, combined with the knowledge that each stimulus in a brief train produces the same increase in calcium. The curve describing the saturation during a train depends primarily upon the affinity of the dye, the increase of calcium per action potential, and the resting calcium levels. Assuming a resting calcium level of 50 nM, simulations in which a single stimulus increases calcium by 300 nM saturate to a degree similar to that observed experimentally.

This method of estimating the magnitude of calcium increases does not depend on knowing the percentage of the fibers that are stimulated and does not require ratio measurements. The key to this approach is to use information provided by dyes with very different calcium affinities. The estimate of 300 nM increase per stimulus is subject to the many uncertainties that accompany the use of Fura-2 within

TABLE 2 Properties of calcium transients produced by single action potentials in different types of presynaptic terminals

Synapse	Presynaptic bouton size	$\Delta[Ca2^+]_i$ per action potential (nM)	Time constant of decay (s)	References
Squid giant synapse	50 × 50 × 750 μm^3			Smith et al. (1993)
Crayfish neuromuscular junction	5–7 μm in diameter	5–10	5	Tank et al. (1991)
Hippocampal granule cell to CA3 pyramidal cell synapse	3–5 μm in diameter	~30	1	Regehr et al. (1994)
Cerebellar granule cell to Purkinje cell synapse	<1 μm in diameter	~300	0.15	This paper

a cell, including changes in the dissociation constant (Konishi et al., 1988) as well as compartmentalization of and incomplete deesterification of dye (Almers and Neher, 1985; Blatter and Wier, 1990).

Comparison with calcium dynamics at other synapses

It is interesting to compare the calcium transients in boutons associated with parallel fibers with those observed in other types of terminals, as summarized in Table 2. Direct comparisons with the squid giant synapse are difficult, as calcium dynamics are dominated, even on rather long time scales, by diffusion in these very long structures. The other synapses included in this table are much smaller, and it is thought that, once calcium equilibrates with the buffers, the return of calcium to resting levels is well approximated by an exponential decay (when $[Ca^{2+}]_i$ is small compared to the K_d of the buffers and the K_p of the pumps). The differences between the terminals are striking. As seen in Table 2, in going from the crayfish neuromuscular junction to the mossy fiber synapse to the parallel fiber synapse, the calcium increase per action potential grows progressively larger and the time constant of decay gets progressively faster. These trends are not unexpected in light of the fact that the ratio of the surface area to the volume of a sphere scales as $(radius)^{-1}$. For a constant buffer concentration and a constant surface density of calcium channels and extrusion mechanisms, the time constant of decay scales as the radius of the terminal, and the magnitude of peak calcium accumulations is inversely proportional to the radius.

We thank Ken Schwartz and Jeremy Dittman for their helpful comments. P.A. received support from training grant NRSA T32GM07753-16. This research was supported by a McKnight Scholars Award and a Klingenstein Fellowship Award in the Neurosciences to W.R.

REFERENCES

Adler, E. M., G. J. Augustine, S. N. Duffy, and M. P. Charlton. 1991. Alien intracellular calcium chelators attenuate neurotransmitter release at the squid giant synapse. *J. Neurosci.* 11:1496–1507.

Almers, W., and E. Neher. 1985. The Ca signal from Fura-2 loaded mast cells depends strongly on the method of dye-loading. *FEBS Lett.* 192: 13–18.

Anderson, K., F. A. Lai, Q.-Y. Liu, E. Rousseau, H. P. Erickson, and G. Meissner. 1989. Structural and functional characterization of the purified cardiac ryanodine receptor-Ca^{2+} release channel complex. *J. Biol. Chem.* 264:1329–1335.

Augustine, G. J., E. M. Adler, and M. P. Charlton. 1991. The calcium signal for transmitter secretion from presynaptic nerve terminals. *Ann. NY Acad. Sci.* 635:365–81.

Baylor, S. M., and S. Hollingworth. 1988. Fura-2 calcium transients in frog skeletal muscle fibres. *J. Physiol.* 403:151–92.

Berlin, J. R., and M. Konishi. 1993. Ca^{2+} transients in cardiac myocytes measured with high and low affinity Ca^{2+} indicators. *Biophys. J.* 65: 1632–47.

Blatter, L. A., and W. G. Wier. 1990. Intracellular diffusion, binding and compartmentalization of the fluorescent calcium indicators indo-1 and Fura-2. *Biophys. J.* 58:1491–1499.

Blundon, J. A., S. N. Wright, M. S. Brodwick, and G. D. Bittner. 1993. Residual free calcium is not responsible for facilitation of neurotransmitter release. *Proc. Natl. Acad. Sci. USA.* 90:9388–9392.

Crank, J. 1975. The Mathematics of Diffusion, 2nd ed. Clarendon Press, Oxford.

Delaney, K. R., and D. W. Tank. 1994. A quantitative measurement of the dependence of short term enhancement on presynaptic residual calcium. *J. Neurosci.* 14:5885–5902.

Delaney, K. R., R. S. Zucker, and D.W. Tank. 1989. Calcium in motor nerve terminals associated with posttetanic potentiation. *J. Neurosci.* 9:3558–3567.

Feller, M. B., K. R. Delaney, and D. W. Tank. 1993. Optical measurements of presynaptic calcium dynamics in frog tectum. *Soc. Neurosci.* Abstr. 19:1125.

Fogelson, A. L., and R. S. Zucker. 1985. Presynaptic calcium diffusion from various arrays of single channels: implications for transmitter release and synaptic facilitation. *Biophys. J.* 48:1003–17.

Fujita, Y., M. Mynlieff, R. T. Dirksen, M.-S. Kim, T. Niidome, J. Nakai, T. Friedrich, N. Iwabe, T. Miyata, T. Furuichi, D. Furutama, K. Mikoshiba, Y. Mori, and K. G. Beam. 1993. Primary structure and functional expression of the ω-conotoxin sensitive N-type calcium channel from rabbit brain. *Neuron.* 10:585–598.

Grynkiewicz, G., M. Poenie, and R. Y. Tsien. 1985. A new generation of Ca^{2+} indicators with greatly improved fluorescence properties. *J. Biol. Chem.* 260:3440–3450.

Hamori, J., and J. Szentagothai. 1964. The "crossing over" synapse: an electron microscope study of the molecular layer in the cerebellar cortex. *Acta Biol. Acad. Sci. Hung.* 15:95–117.

Herrington, J., and R. J. Bookman. 1994. Pulse Control V4.3: IGOR XOPs for Patch Clamp Data Acquisition, and Capacitance Measurements. University of Miami, Miami, FL.

Heidelberger, R., C. Heinemann, E. Neher, and G. Matthews. 1994. Calcium dependence of the rate of exocytosis in a synaptic terminal. *Nature.* 371: 513–515.

Hillyard, D. R., V. D. Monje, I. M. Mintz, B. P. Bean, L. Nadasdi, J. Ramachandran, G. Miljanich, A. Azimi-Zoonooz, J. M. McIntosh, L. J. Cruz, J. S. Imperial, and B. M. Olivera. 1992. A new conus peptide ligand for mammalian presynaptic Ca^{2+} channels. *Neuron.* 9:69–77.

Hinkle, P. M., E. Shanshala, and E. J. Nelson. 1992. Measurement of intracellular cadmium with fluorescent dyes: further evidence for the role of calcium channels in cadmium uptake. *J. Biol. Chem.* 267:25553–25559.

Hollingworth, S., A. B. Harkins, N. Kurebayashi, M. Konishi, and S. M.

Baylor. 1992. Excitation-contraction coupling in intact frog skeletal muscle fibers injected with mmolar concentrations of Fura-2. *Biophys. J.* 63:224–234.

Honore, T., S. N. Davies, J. Drejer, E. J. Fletcher, P. Jacobsen, D. Lodge, and F. E. Nielsen. 1988. Quinoxalinediones: potent competitive non-NMDA glutamate receptor antagonists. *Science.* 241:701–703.

Iatridou, H., E. Foukaraki, M. A. Kuhn, E. M. Marcus, R. P. Haugland, and H. E. Katerinopoulos. 1994. The development of a new family of intracellular calcium probes. *Cell Calcium.* 15:190–198.

Kao, J. P. Y., and R. Y. Tsien. 1988. Ca^{2+} binding kinetics of Fura-2 and azo-1 from temperature-jump relaxation measurements. *Biophys. J.* 53: 635–639.

Katz, B., and R. Miledi. 1968. The role of calcium in neuromuscular facilitation. *J. Physiol.* 203:459–487.

Klein, M. G., B. J. Simon, G. Szucs, and M. F. Schneider. 1988. Simultaneous recording of calcium transients in skeletal muscle using high- and low- affinity calcium indicators. *Biophys. J.* 53:971–988.

Konishi, M., and J. R. Berlin. 1993. Ca transients in cardiac myocytes measured with a low affinity fluorescent indicator, furaptra. *Biophys. J.* 64:1331–1343.

Konishi, M., S. Hollingworth, A. B. Harkins, and S. M. Baylor. 1991. Myoplasmic calcium transients in intact frog skeletal muscle fibers monitored with the fluorescent indicator furaptra. *J. Gen. Physiol.* 97:271–301.

Konishi, M., A. Olson, S. Hollingworth, and S. M. Baylor. 1988. Myoplasmic binding of Fura-2 investigated by steady-state fluorescence and absorbance measurements. *Biophys. J.* 54:1089–1104.

Llinas, R., M. Sugimori, and R. B. Silver. 1992. Microdomains of high calcium concentration in a presynaptic terminal. *Science.* 256:677–679.

Mintz, I. M., M. E. Adams, and B. P. Bean. 1992. P-type calcium channels in rat central and peripheral neurons. *Neuron.* 9:85–95.

Neher, E., and G. J. Augustine. 1992. Calcium gradients and buffers in bovine chromaffin cells. *J. Physiol.* 450:273–301.

Nowycky, M. C., and M. J. Pinter. 1993. Time courses of calcium and calcium-bound buffers following calcium influx in a model cell. *Biophys. J.* 64:77–91.

Palay, S. L., and V. Chan-Palay. 1974. Cerebellar Cortex. Springer-Verlag, New York.

Palkovits, M., P. Magyar, and J. Szentagothai. 1971. Quantitative histological analysis of the cerebellar cortex in the cat. III. Structural organization of the molecular layer. *Brain Res.* 34:1–18.

Raju, B., E. Murphy, L. A. Levy, R. D. Hall, and R. E. London. 1989. A fluorescent indicator for measuring cytosolic free magnesium. *Am. J. Physiol.* 256:C540-C548.

Regehr, W. G., K. R. Delaney, and D. W. Tank. 1994. The role of presynaptic calcium in short-term enhancement at the hippocampal mossy fiber synapse. *J. Neurosci.* 14:523–537.

Regehr, W. G., and D. W. Tank. 1991a. The maintenance of LTP at hippocampal mossy fiber synapses is independent of sustained presynaptic calcium. *Neuron.* 7:451–459.

Regehr, W. G., and D. W. Tank. 1991b. Selective Fura-2 loading of presynaptic terminals and nerve cell processes by local perfusion in mammalian brain slices. *J. Neurosci. Methods.* 37:111–119.

Regehr, W. G., and D. W. Tank. 1992. Calcium concentration dynamics produced by synaptic activation of CA1 hippocampal pyramidal cells. *J. Neurosci.* 12:4202–4223.

Robitaille, R., E. M. Adler, and M. P. Charlton. 1990. Strategic location of calcium channels at transmitter release sites of frog neuromuscular synapses. *Neuron.* 5:773–779.

Sala, F., and C. A. Hernandez. 1990. Calcium diffusion modeling in a spherical neuron: relevance of buffering properties. *Biophys. J.* 57:313–324.

Simon, S. M., and R. R. Llinas. 1985. Compartmentalization of the submembrane calcium activity during calcium influx and its significance in transmitter release. *Biophys. J.* 48:485–498.

Smith, S. J., J. Buchanan, L. R. Osses, M. Charlton, and G. J. Augustine. 1993. The spatial distribution of calcium signals in squid presynaptic terminals. *J. Physiol.* 472:573–593.

Swandulla, D., M. Hans, K. Zipser, and G. J. Augustine. 1991. Role of residual calcium in synaptic depression and posttetanic potentiation: fast and slow calcium signaling in nerve terminals. *Neuron.* 7:915–926.

Tank, D. W., W. G. Regehr, and K. R. Delaney. 1991. Modeling a synaptic chemical computation: the buildup and decay of presynaptic calcium. *Soc. Neurosci.* Abstr. 17:578.

Thastrup, O., P. J. Cullen, B. K. Drobak, M. R. Hanley, and A. P. Dawson. 1990. Thapsigargin, a tumor promoter, discharges intracellular Ca^{2+} stores by specific inhibition of the endoplasmic reticulum Ca^{2+}-ATPase. *Proc. Natl. Acad. Sci. USA.* 87:2466–2470.

Williams, M. E., P. F. Brust, D. H. Feldman, S. Patthi, S. Simerson, A. Maroufi, A. F. McCue, G. Velicelebi, S. B. Ellis, and M. M. Harpold. 1992. Structure and functional expression of a ω-conotoxin-sensitive human N-type calcium channel. *Science.* 257:389–395.

Winslow, J. L., S. N. Duffy, and M. P. Charlton. 1994. Homosynaptic facilitation of transmitter release in crayfish is not affected by mobile calcium chelators: implications for the residual ionized calcium hypothesis from electrophysiological and computational analyses. *J. Neurophysiol.* 72:1769–1793.

Wu, L. G., and P. Saggau 1994a. Adenosine inhibits evoked synaptic transmission primarily by reducing presynaptic calcium influx in area CA1 of hippocampus. *Neuron.* 12:1139–1148.

Wu, L. G., and P. Saggau. 1994b. Presynaptic calcium is increased during normal synaptic transmission and paired-pulse facilitation, but not in long-term potentiation in area CA1 of hippocampus. *J. Neurosci.* 14: 645–654.

Yamada, W. M., and R. S. Zucker. 1992. Time course of transmitter release calculated from simulations of a calcium diffusion model. *Biophys. J.* 61:671–682.